Journal of Fundamental and Applied Research **Vol. 4**, Issue 1 (2024) **20240004**

Received: 06 March 2024 / Accepted: 29 March 2024
Published online: 29 March 2024
© 2024 The Author(s)

Impact of higher harmonics in d-wave gap symmetry on superfluid density in cuprate superconductors

O. Ganiev,[1, 2, 3, *] B. Yavidov,[4] M. Fayzullaeva,[3] and Z. Rakhmonov[5]

[1]*New Uzbekistan University, 100007 Tashkent, Uzbekistan*
[2]*Institute of Nuclear Physics, AS RUz, 100214 Tashkent, Uzbekistan*
[3]*National University of Uzbekistan, 100174 Tashkent, Uzbekistan*
[4]*Nukus State Pedagogical Institute named after Ajiniyaz, 230105 Nukus, Karakalpakstan, Uzbekistan*
[5]*Engineering Physics Institute, Samarkand State University, 140104 Samarkand, Uzbekistan*

Abstract. The nature of the pairing state in high-temperature cuprate superconductors continues to be a central question in condensed matter physics. While a d-wave symmetry for the superconducting gap is widely accepted, a complete understanding of its origin and consequences remains elusive. In this paper we examined the implications of an extended d-wave pairing scenario on the temperature dependence of the superfluid density, a key property reflecting the concentration of Cooper pairs. Employing a theoretical framework based on an extended d-wave gap symmetry, we use the Chandrasekhar and Einzel approach to calculate the temperature-dependent superfluid density in cuprate superconductors. Our calculations incorporate the self-consistent determination of the superconducting gap, taking into account the extended d-wave symmetry. We compare our theoretical predictions with experimental data obtained from various cuprate materials, finding excellent agreement across different temperature regimes. Our results contribute to a deeper understanding of the complex interplay between pairing symmetry and superconducting properties in cuprate superconductors.

Keywords: superconducting cuprates, superconducting gap symmetry, superfluid density, condensed matter, quasiparticle excitations.

I. INTRODUCTION

The fascinating realm of high-temperature cuprate superconductors is marked by a central mystery: the precise nature of the pairing mechanism responsible for their remarkable properties. A key aspect of this puzzle lies in the symmetry of the superconducting gap, which dictates the allowed quasiparticle excitations and ultimately governs superconducting behavior of the material [1]. While extensive experimental evidence points towards a dominant d-wave symmetry for the gap in cuprates, the full picture is far from simple, with intriguing deviations and complexities emerging in different cuprate families and doping regimes.

Powerful techniques such as angle-resolved photoemission spectroscopy (ARPES) have confirmed the d-wave nature of the gap in numerous cuprates, revealing its characteristic angular dependence with nodes along the diagonals of the crystal lattice. However, deviations from the idealized d-wave picture have been observed, suggesting the presence of more intricate gap structures in certain cuprates. These deviations manifest in various ways, including subtle distortions of the gap function and the emergence of additional gap components beyond the standard d-wave form [2–4].

The d-wave symmetry manifests as an angular dependence of the gap, reaching its maximum value along the diagonals of the crystal lattice. Hole-doped cuprates, for instance, exhibit a gap described by the equation $\Delta = \Delta_0 \cos(2\theta)$, as initially observed in ARPES experiments [5, 6]. Yet, even within hole-doped cuprates, deviations from the typical $d_{x^2-y^2}$ form have been identified in Bi-based compounds [7]. The situation becomes even more intricate in electron-doped cuprates, where the gap modulation on the Fermi surface requires additional terms beyond the standard d-wave form [8]. Recent research by Khasanov et al. [9] employed magnetization measurements to study the temperature dependence of the magnetic field penetration depth in the electron-doped superconductor $Sr_{0.9}La_{0.1}CuO_2$. Their analysis, using a two-gap model with mixed $s + d$-wave symmetry,

* Corresponding author: ganiev@inp.uz

aligns with previous studies suggesting a distinct angular dependence of the gap function in electron-doped cuprates, deviating from the conventional $\Delta_0 \cos(2\theta)$ form [10–13]. These findings highlight the need for a deeper understanding of the nuances of the superconducting gap and its influence on cuprate superconductivity.

In this study, we delve into the implications of an extended d-wave pairing scenario, where higher angular harmonics of the d-wave gap are considered. By employing the Chandrasekhar and Einzel approach, we aim to meticulously calculate the temperature dependence of the superfluid density, a crucial quantity reflecting the density of superconducting charge carriers. This will enable precise fitting of experimental data, offering valuable insights into the complex interplay between gap symmetry and superconductivity in these remarkable materials.

II. SUPERFLUID DENSITY

Cuprate superconductors, renowned for their high critical temperatures, exhibit unique complexities due to the unconventional d-wave symmetry of their superconducting gap. Unlike conventional s-wave superconductors with a uniform distribution of Cooper pairs, the d-wave symmetry leads to an anisotropic pairing, where the Cooper pair density varies depending on the direction within the crystal lattice. This direction-dependent superfluid density directly influences of the superconductor ability to carry current, with higher superfluid density corresponding to directions of stronger superconductivity.

On the whole cuprate superconductors exhibit complex behavior and their superfluid density is affected by several factors such as temperature, doping level, crystal structure, magnetic field, anisotropy, competing orders, and pseudogap phase. The following factors contribute to the change in superfluid density in cuprate superconductors:

- **Temperature:** As the temperature increases, the superfluid density decreases. As the temperature approaches the critical point T_c, where superconductivity is lost, the number of Cooper pairs decreases, which leads to a decrease in superfluid density.
- **Doping level:** To enhance their T_c, cuprate superconductors are doped with impurities, altering their concentration. Modifying the doping level can impact the count of charge carriers and adjust the quantity of Cooper pairs, thus affecting superfluid density. The optimal doping level for achieving the highest T_c and superfluid density varies among different cuprate superconductors.
- **Crystal structure:** Cuprate superconductors possess intricate crystal structures with copper-oxide layers. Various cuprate compounds exhibit diverse crystal arrangements of copper and oxygen atoms. These structural disparities influence electronic properties, such as density of states and Cooper pair formation, which consequently affect superfluid density.
- **Magnetic field:** The application of a magnetic field can alter the superfluid density in cuprate superconductors. Low magnetic fields have minimal impact on superfluid density. However, at higher magnetic fields, the number of Cooper pairs may decrease, leading to a reduction in superfluid density.
- **Anisotropy:** Cuprate superconductors often exhibit strong anisotropic behavior, meaning that their properties vary depending on the direction in the crystal lattice. This anisotropy can affect the mobility of charge carriers and Cooper pairs, influencing the superfluid density in different directions.
- **Competing orders:** Cuprates often exhibit competing electronic orders, such as charge density waves or spin density waves, which can interact with superconductivity and influence the superfluid density.
- **Pseudogap phase:** The enigmatic pseudogap phase, observed in the underdoped regime of cuprates, presents further challenges in understanding the behavior of superfluid density and its connection to the superconducting mechanism.

By carefully considering these multifaceted factors, researchers strive to unravel the complexities of superfluid density in cuprate superconductors, paving the way for further advancements in high-temperature superconductivity.

This section investigates the behavior of superfluid density, a key property governing the electrodynamics of superconductors, with a particular focus on singlet pairing states where electrons form Cooper pairs with opposite spins. We employ the powerful quasi-classical formalism developed by Chandrasekhar and Einzel [14], which provides a semiclassical framework to analyze the supercurrent response to an applied magnetic field. By considering the intricate details of the Fermi surface topology and the energy gap structure, we can extract crucial information about the penetration depth, a characteristic length scale dictating of the magnetic field penetration into the superconductor. This analysis allows us to elucidate the intricate relationship between supercurrent flow, band structure, and the superconducting energy gap, paving the way for a deeper understanding of the electrodynamic response in various superconducting materials.

In an anisotropic superconductor, and within the London approximation where the London penetration depth λ is greater than the coherence length ξ ($\lambda > \xi$), the supercurrent density $\mathbf{J}$ is related to the vector potential $\mathbf{A}$ through a response tensor $\mathbb{T}$. This

 Copyright © 2024

relationship is mathematically expressed as:

$$\mathbf{J} = -\mathbb{T}\mathbf{A}, \tag{1}$$

The response tensor $\mathbb{T}$ is defined as follows:

$$\mathbb{T} = \frac{e^2}{4\pi^3 c}\int d^3k \left(-\frac{\partial n_k}{\partial \varepsilon_k} + \frac{\partial f(E_k)}{\partial E_k}\right)(\mathbf{v}_k\mathbf{v}_k). \tag{2}$$

Here, e is the elementary charge, c is the speed of light, and $f(E_k) = (e^{E_k/k_BT}+1)^{-1}$ is the Fermi-Dirac distribution function. The integral is taken over the three-dimensional momentum space with $\mathbf{v}_k$ representing the velocity of electrons. The response tensor $\mathbb{T}$ essentially characterizes how the supercurrent density responds to the vector potential in the presence of anisotropy in the superconductor.

The penetration depth components along specific directions relative to the crystalline axes can be calculated using the relationship:

$$\lambda_{ii} = \left(\frac{c}{4\pi T_{ii}}\right)^{1/2}, \quad i = x, y, z \tag{3}$$

It is important to note that the λ_{ii} values are not the components of a vector or a tensor; instead, they represent the distinct penetration depths concerning the crystalline axes.

On the other hand, the effective mass can be defined as:

$$m_{ii} = \frac{ne^2}{cT_{ii}}, \tag{4}$$

This definition leads to the familiar London relation:

$$\lambda_{ii} = \left(\frac{m_{ii}c^2}{4\pi^2}\right)^{1/2}. \tag{5}$$

Consider now the structure of the response tensor, $\mathbb{T}$, shown in equation (2). The response tensor, denoted as $\mathbb{T}$, can be divided into two distinct terms known as the diamagnetic term ($\mathbb{T}_D$) and the paramagnetic term ($\mathbb{T}_P$). This can be expressed as:

$$\mathbb{T} = \mathbb{T}_D - \mathbb{T}_P. \tag{6}$$

The diamagnetic term ($\mathbb{T}_D$) and paramagnetic term ($\mathbb{T}_P$) of the response tensor are associated with the properties of the material in its normal state and superconducting state, respectively. They are defined as:

$$\mathbb{T}_D = \frac{e^2}{4\pi^3 c}\int d^3k \left(-\frac{\partial n_k}{\partial \varepsilon_k}\right)(\mathbf{v}_k\mathbf{v}_k) \tag{7}$$

and

$$\mathbb{T}_P = \frac{e^2}{4\pi^3 c}\int d^3k \left(-\frac{\partial f(E_k)}{\partial E_k}\right)(\mathbf{v}_k\mathbf{v}_k), \tag{8}$$

To simplify the calculations, certain approximations are made, assuming that the derivatives in equations (7) and (8) are significant only when $|\varepsilon_k - \mu| \lesssim \Delta(k)$ and that $\Delta(k) << \mu$. This allows us to replace $\mathbf{v}_k\mathbf{v}_k$ with its value at $\varepsilon_k = \mu$, denoted as $\mathbf{v}_F\mathbf{v}_F$. Additionally, we can make the substitution:

$$d^3k \longrightarrow \frac{dS_F d\varepsilon_k}{\hbar|\mathbf{v}_k|} \tag{9}$$

where dS_F is a constant energy surface element and $\mathbf{v}_k$ is the magnitude of the Fermi velocity.

Based on these approximations, we arrive at simplified expressions for $\mathbb{T}_D$ and $\mathbb{T}_P$:

$$\mathbb{T}_D = \frac{e^2}{4\pi^3\hbar c}\oint dS_F \int_0^\infty d\varepsilon_k \left(-\frac{\partial n_k}{\partial \varepsilon_k}\right)\frac{\mathbf{v}_k\mathbf{v}_k}{|\mathbf{v}_F|} \cong \frac{e^2}{4\pi^3\hbar c}\oint dS_F \frac{\mathbf{v}_k\mathbf{v}_k}{|\mathbf{v}_F|} \tag{10}$$

Copyright © 2024

and

$$\mathbb{T}_P \;\cong\; 2\cdot\frac{e^2}{4\pi^3\hbar c}\oint dS_F\frac{\mathbf{v}_k\mathbf{v}_k}{|\mathbf{v}_F|}\int\limits_{\Delta(k)}^{\infty}dE_k\left(-\frac{\partial f(E_k)}{\partial E_k}\right)\frac{E_k}{\sqrt{E_k^2-\Delta^2(k)}}. \tag{11}$$

where k_B is Boltzmann's constant.

The analysis of equations (10) and (11) leads to the following conclusions:

(i) $\mathbb{T}_D$ remains temperature-independent and reflects the anisotropy of ε_k, or equivalently of the Fermi surface.

(ii) As $T\longrightarrow 0$, $\mathbb{T}_P\longrightarrow 0$ and as $T\longrightarrow T_c$, $\mathbb{T}_P\longrightarrow\mathbb{T}_D$.

(iii) If $\Delta(k)$ is isotropic, $\mathbb{T}_P$ exhibits temperature-independent anisotropy, with the same anisotropy as $\mathbb{T}_D$.

(iv) If $\Delta(k)$ is anisotropic, the anisotropy of $\mathbb{T}_P$ depends on both the anisotropy of ε_k and $\Delta(k)$, and it is also temperature-dependent.

The normalized superfluid density, denoted as ρ_s, represents the ratio of the concentration of superconducting electrons to the total concentration of available charge. It is related to the penetration depth by the equation:

$$\rho_s=\frac{n_s(T)}{n_s(0)}=\left(\frac{\lambda(0)}{\lambda(T)}\right)^2 \tag{12}$$

where $n_s(T)$ and $n_s(0)$ are the densities of superconducting electrons at temperature T and $T=0$ (absolute zero), respectively, and $\lambda(T)$ and $\lambda(0)$ are the penetration depths at temperature T and $T=0$.

The normalized superfluid density components, denoted as ρ_{ii}, can be calculated using the following equations:

$$\rho_{ii}=\frac{\lambda_{ii}^2(0)}{\lambda_{ii}^2(T)}=\frac{\mathbb{T}_{ii}(T)}{\mathbb{T}_{ii}(0)}, \tag{13}$$

The expression for $\mathbb{T}_{ij}$, which is a component of the response tensor, can be written as

$$\mathbb{T}_{ij} \;=\; \frac{e^2}{4\pi^3\hbar c}\oint_{FS}dS_F\left[\frac{\mathrm{v}_F^i\mathrm{v}_F^j}{|\mathbf{v}_F|}\left(1+2\int\limits_{\Delta(k)}^{\infty}\frac{\partial f(E)}{\partial E}\frac{N(E)}{N(0)}dE\right)\right] \tag{14}$$

where the subscripts i, j denote the directions of the current and vector potential, v_F^i and v_F^j are components of the Fermi velocity vector $\mathbf{v}_F$, and $N(E)$ is the quasiparticle density of states. The quasiparticle energy spectrum is given by $E=\sqrt{\varepsilon_k^2-\Delta^2(k)}$, where ε_k is the excitation energy with respect to the Fermi level (ε_F).

These equations allow us to calculate the superfluid density in terms of the superconducting gap (Δ) and the single particle excitation energy (ε_F) with respect to the Fermi level for a general Fermi surface geometry. Equation (14) establishes the connection between the experimentally measured penetration depth and the microscopic superconducting state. For two general cases of pairing symmetry, we can obtain expressions for the normalized superfluid density.

For isotropic s-wave pairing with both two-dimensional (2D) cylindrical and three-dimensional (3D) spherical Fermi surfaces, the integral in equation (14) can be simplified, resulting in:

$$\rho_s \;=\; \left(\frac{\lambda(0)}{\lambda(T)}\right)^2=1-\frac{1}{2\pi k_BT}\int\limits_0^{\infty}\mathrm{sech}^2\left(\frac{\sqrt{\varepsilon^2+\Delta^2(T)}}{2k_BT}\right)d\varepsilon. \tag{15}$$

For d-wave cuprate superconductors with a 2D cylindrical Fermi surface, the temperature dependence of the normalized superfluid density can be simplified to:

$$\rho_s \;=\; 1-\frac{1}{2\pi k_BT}\int\limits_0^{2\pi}\begin{pmatrix}\cos^2(\theta)\\ \sin^2(\theta)\end{pmatrix}\int\limits_0^{\infty}\mathrm{sech}^2\left(\frac{\sqrt{\varepsilon^2+\Delta_{ed}^2(T,\theta)}}{2k_BT}\right)d\varepsilon d\theta. \tag{16}$$

Here $\Delta_{ed}(T,\theta)$ represents the extended d-wave gap function as a function of temperature T and angle θ in momentum space. In the extended d-wave symmetry, the gap has an additional $\cos(6\theta)$ term, which can be written as:

$$\Delta_{ed}(T,\theta) \;=\; \Delta(T)\,g(\theta)=\Delta(T)\left[B\cos(2\theta)+(1-B)\cos(6\theta)\right] \tag{17}$$

 Copyright © 2024

B is the gap anisotropy parameter. The parameter B provides flexibility in tuning the relative contributions of the $\cos(2\theta)$ and $\cos(6\theta)$ components, enabling the model to adapt to different materials and doping levels. This form of the d-wave gap function was introduced in ARPES studies to describe the deviation of the superconducting gap from the monotonic $d_{x^2-y^2}$ wave symmetry in Bi-based cuprates [7]. It characterizes the modulation of the gap magnitude on the Fermi surface [8].

To calculate the superfluid density, we need to determine the temperature dependence of the gap magnitude. This is done through solving the self-consistent gap equation, which relies on the pairing symmetry and the specific characteristics of the Fermi surface. The self-consistent gap equation can be expressed as follows:

$$\int_0^{2\pi}\int_0^{\infty} g(\theta)^2 \left(\frac{\tanh\left[\frac{\sqrt{\varepsilon^2+\Delta_{ed}^2(T,\theta)}}{2k_BT}\right]}{\sqrt{\varepsilon^2+\Delta_{ed}^2(T,\theta)}} - \frac{\tanh\left[\frac{\varepsilon}{2}\right]}{\varepsilon} \right) d\varepsilon d\theta = 0. \tag{18}$$

In cuprate superconductors, the superfluid density is a measure of the density of Cooper pairs that carry the supercurrent. Especially, the superfluid density is closely related to the number of Cooper pairs of electrons that are responsible for the superconducting state. At temperatures below T_c, where superconductivity occurs, the superfluid density is expected to be nonzero and proportional to the density of Cooper pairs.

III. RESULTS AND DISCUSSION

The understanding of the pairing state in high-T_c superconductors is still incomplete, even though numerous experimental findings strongly support the existence of a d-wave gap. Both experimental and theoretical investigations consistently highlight the significance of determining the pairing symmetry to explore the effects of gaps on the behavior of superfluid density.

Our investigation begins by examining the nuanced behavior of the d-wave gap magnitude as it varies around the Fermi surface. In Fig. 1, we present a comparative analysis of this variation for several representative cases of cuprate superconductors. These cases encompass:

- **Underdoped Bi2212:** Characterized by a critical temperature ($T_c = 80$ K) and a gap anisotropy parameter ($B = 1$), as reported by Mesot et al. [7].
- **Overdoped Bi2212:** Also with a $T_c = 80$ K, but exhibiting a reduced gap anisotropy with $B = 0.88$ [7]. Optimally doped Bi2201: This compound, $(Bi,Pb)_2(Sr,La)_2CuO_{6+\delta}$, has a $T_c = 35$ K and a gap anisotropy of $B = 0.78$ [11].
- **Optimally doped PLCCO:** $Pr_{0.89}LaCe_{0.11}CuO_4$ exhibits a $T_c = 26$ K and a more pronounced gap anisotropy with $B = 1.43$ [8].

The variations in the d-wave gap magnitude for these cases are visually represented using polar plots, allowing for a clear comparison of their angular dependence. We note that the ratio of the maximum gap value to the critical temperature, $\Delta(0)/T_c$, varies among these materials, taking values of 2.23 for underdoped Bi2212, 2.14 for overdoped Bi2212, 2.23 for optimally doped Bi2201, and 1.55 for optimally doped PLCCO.

Figure 2a shows the superconducting energy gap Δ of the above compounds as a function of normalized temperature (T/T_c) for the extended d-wave gap obtained from numerical solutions of the self-consistent gap equations. Taking a model d-wave gap, $\Delta_{ed}(T,\theta) = \Delta(T)[B\cos(2\theta) + (1-B)\cos(6\theta)]$, we have found that the temperature evolution of the extended d-wave gaps.

To create a comprehensive reference, we have conducted calculations for the ratio $\Delta(0)/T_c$ over a wider range of B values, specifically ranging $0 \leq B \leq 2$. These calculations were carried out using equation (18) by numerically solving the self-consistency equation for the d-wave gap at $T = 0$. The results obtained are shown in Fig. 2b. The curve in Fig. 2b is surprisingly nonmonotonic for $B < 1$, but changes smoothly for $B \geq 1$. The red point in the Fig. 2b, corresponding to $B = 1$, signifies the presence of nodal d-wave superconductivity.

Further, the second result is the temperature dependence of the normalized superfluid density, calculated with the extended d-wave gap, as if all of this contributed to superconductivity. These dependencies are presented in Fig. 3 from which one can see that the superfluid density dependencies for the nodal $d-$wave gap and an extended $d-$wave gap cases are differ significantly. While this may in principle exist, this behavior is unlikely and implies that the spectral gap measured by ARPES in cuprate superconductors is a combination of a nodal d-wave ($B = 1$) superconducting gap and a pseudogap that does not contribute to condensation. However, the pseudogap affects the spectral density of quasiparticles, and this must be taken into account [8, 15–18] when calculating the superfluid density. To reliably estimate the density of a superfluid density, accurate measurements of the temperature-dependent penetration depth as well as its value at zero temperature are required.

For $B \geq 1$, the superfluid density exhibits normal convex behavior, while for $B < 1$, the behavior is concave. As proof of this, for electron-doped cuprates, our results show that the behavior differs significantly from that of hole-doped analogs, and the

Copyright © 2024

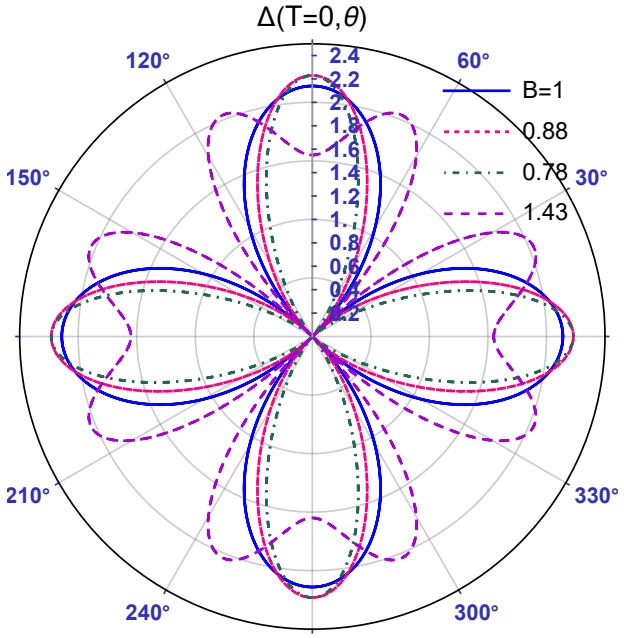


FIG. 1. Angular variation of the d-wave gap magnitudes for different cuprates: underdoped Bi-2212 ($B = 0.88$), overdoped Bi-2212 ($B = 1$), optimally doped Bi-2201 ($B = 0.78$), and PLCCO ($B = 1.43$). The calculations are performed using equation (17), and the results are obtained around the Fermi surface for each respective case.

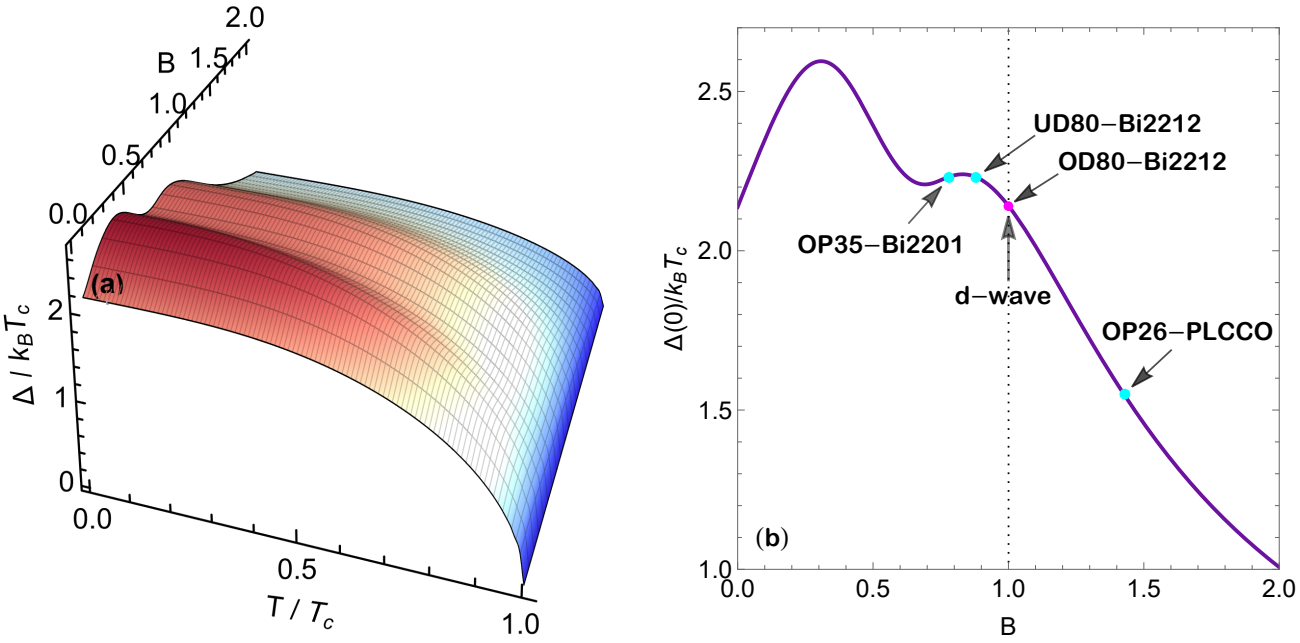


FIG. 2. (a) The superconducting energy gap as a function of normalized temperature (T/T_c) and parameter B, obtained from numerical solutions of the self-consistent gap equations. (b) The ratio of the energy gap at zero temperature to the critical temperature, $\Delta(0)/T_c$, plotted as a function of B.

non-monotonic gap creates a superfluid density with $B > 1$, which indicates a significant contribution from the second harmonic of the $d_{x^2-y^2}$ gap. We have demonstrated that the non-monotonic gap function, equation (17), should lead to an unusual sub-linear temperature dependence of ρ_s. It is quite possible that such an unusual gap structure is the result of the interference of a superconducting gap and a pseudogap. In this case, the superfluid density is determined only by the superconducting gap, and measurements of the penetration depth will be very useful for elucidating physics.

Copyright © 2024

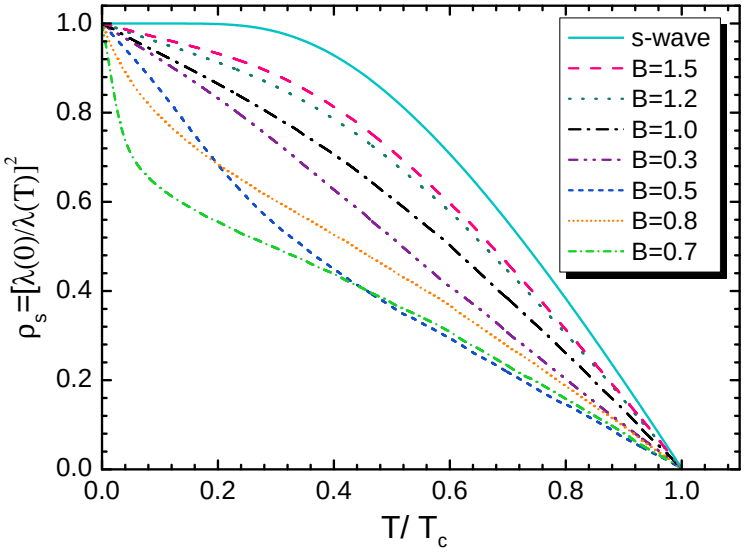


FIG. 3. The temperature dependence of the normalized superfluid density calculated for nodal d-wave gap (for $B = 1.0$) and various values of B for non-monotonic d-wave gaps.

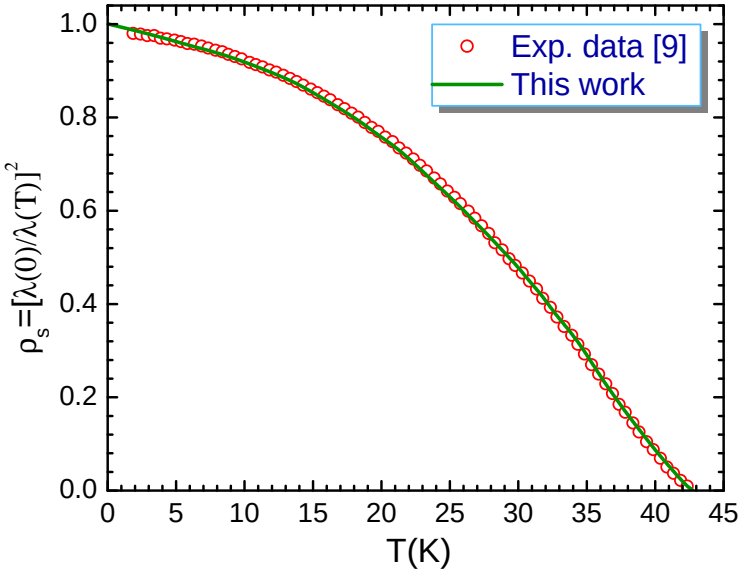


FIG. 4. Comparison of the calculated results for the normalized superfluid density ρ_s (solid line) with experimental AC susceptibility data (open circles) reported by Khasanov et al. [9] for the electron-doped cuprate superconductor $Sr_{0.9}La_{0.1}CuO_2$.

In Fig. 4, we compare our calculated ρ_s as a function of temperature with recent experimental AC susceptibility data given by Khasanov et al. [9] for electron-doped cuprate superconductor $Sr_{0.9}La_{0.1}CuO_2$. One feature of ρ_s in Fig. 4 is that the symmetry of the gap in electron-doped cuprates changes from a pure d-wave to an extended d-wave. The reason for this change is that the superfluid density in the superconducting state is especially sensitive to changes in anisotropy (i.e., to changes in parameter $B = 1.43$). Furthermore, it is very important to note that at low temperatures ρ_s linear depends on the temperature.

Next, the results of calculation of the superfluid density with experimental data in single layer tetragonal compound $Tl_2Ba_2CuO_{6+\delta}$ (Tl-2201) at almost optimally doping ($T_c = 78$ K) [19], in 15% Y-doped Bi-2212 (i.e., $Bi_{2.1}Sr_{1.9}Ca_{0.85}Y_{0.15}Cu_2O_{8+\delta}$) at optimal doping, $\delta = 0.16$ (maximum $T_c = 90$ K) [20], and in pure Bi-2212 ($T_c = 93$ K) [21], respectively. Figure 5 shows the results of the d-wave calculations (solid lines, equation (16)). Symbols show the experimental data. To calculate the temperature dependence of the superfluid density, the superconducting gap parameter is obtained from the numerical solution of the self-consistent gap equation (18) with extended d-wave symmetry. Thus, for optimally doped Tl-2201, we take the value of parameter B equal to 0.9; $B = 0.88$ for 15% Y-doped Bi-2212; and $B = 1.0$ for pure Bi-2212, respectively. A characteristic feature of this theory is linear behavior of ρ_s at low temperatures. Here, the coincidence of calculations and experimental data

Copyright © 2024

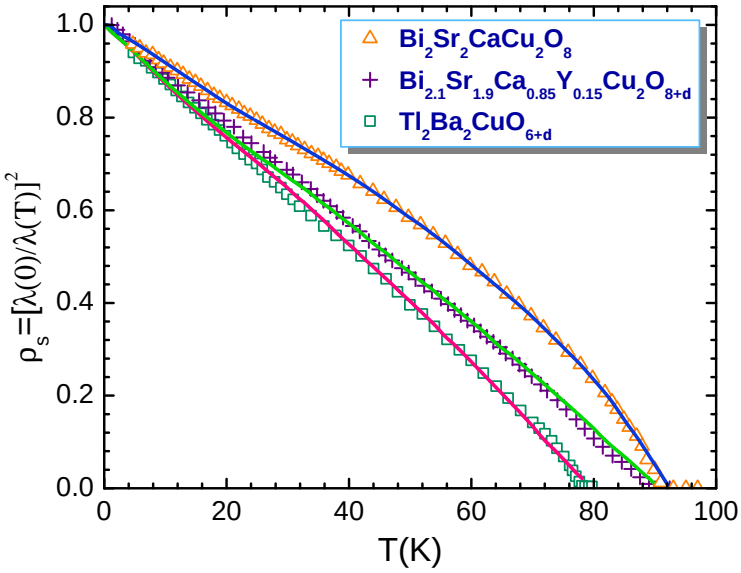


FIG. 5. The normalized superfluid density plotted as a function of temperature. Symbols: experimental data in single layer tetragonal compound $Tl_2Ba_2CuO_{6+\delta}$ ($T_c = 78$ K) [19], experimental AC susceptibility data in $Bi_{2.1}Sr_{1.9}Ca_{0.85}Y_{0.15}Cu_2O_{8+\delta}$ at optimal doping, $\delta = 0.16$ (maximum $T_c = 90$ K) [20] and in $Bi_2Sr_2CaCu_2O_8$ ($T_c = 93$ K)[21]. The solid lines represent the results of the d-wave calculations.

can be considered as proof of d-wave pairing.

IV. CONCLUSIONS

In summary, this study has meticulously analysed the intricate interplay between the pairing symmetry of the superconducting gap and the resulting superfluid density. By using a self-consistent gap equation specifically formulated for various pairing symmetries, we have successfully shown the temperature evolution of the extended d-wave gap, $\Delta_{ed}(T,\theta)$. Employing this gap structure in conjunction with generalized BCS-like expressions encompassing higher angular harmonics, we have subsequently calculated the superfluid density, $\rho_s(T)$. The validity and effectiveness of these theoretical tools have been carefully tested against experimental data acquired from d-wave superconductors. Our results demonstrate the strength and applicability of the Chandrasekhar and Einzel approach when d-wave gap is extended with higher angular harmonics. The theoretical framework successfully captures the nuanced temperature dependence of ρ_s observed in experiments, including the concave and linear behavior at low temperatures, as well as the non-linear trends exhibited at higher temperatures. This remarkable agreement between theoretical predictions and experimental observations strongly suggests that the extended d-wave gap, incorporating higher angular harmonics, provides an accurate and comprehensive description of the superfluid density in cuprate superconductors.

REFERENCES

[1] C. C. Tsuei and J. R. Kirtley, Rev. Mod. Phys. **72**, 969 (2000).
[2] N. Bickers and D. Scalapino, Annals of Physics **193**, 206 (1989).
[3] J. Annett, N. Goldenfeld, and S. R. Renn, Phys. Rev. B **43**, 2778 (1991).
[4] P. Monthoux, A. V. Balatsky, and D. Pines, Phys. Rev. Lett. **67**, 3448 (1991).
[5] Z.-X. Shen, D. S. Dessau, B. O. Wells, D. M. King, W. E. Spicer, A. J. Arko, D. Marshall, L. W. Lombardo, A. Kapitulnik, P. Dickinson, S. Doniach, J. DiCarlo, T. Loeser, and C. H. Park, Phys. Rev. Lett. **70**, 1553 (1993).
[6] H. Ding, M. R. Norman, J. C. Campuzano, M. Randeria, A. F. Bellman, T. Yokoya, T. Takahashi, T. Mochiku, and K. Kadowaki, Phys. Rev. B **54**, R9678 (1996).

 Copyright © 2024

[7] J. Mesot, M. R. Norman, H. Ding, M. Randeria, J. C. Campuzano, A. Paramekanti, H. M. Fretwell, A. Kaminski, T. Takeuchi, T. Yokoya, T. Sato, T. Takahashi, T. Mochiku, and K. Kadowaki, Phys. Rev. Lett. **83**, 840 (1999).
[8] T. Kondo, T. Takeuchi, A. Kaminski, S. Tsuda, and S. Shin, Phys. Rev. Lett. **98**, 267004 (2007).
[9] R. Khasanov, A. Shengelaya, R. Brütsch, and H. Keller, Condensed Matter **5** (2020), 10.3390/condmat5030050.
[10] G. Blumberg, A. Koitzsch, A. Gozar, B. S. Dennis, C. A. Kendziora, P. Fournier, and R. L. Greene, Phys. Rev. Lett. **88**, 107002 (2002).
[11] H. Matsui, K. Terashima, T. Sato, T. Takahashi, M. Fujita, and K. Yamada, Phys. Rev. Lett. **95**, 017003 (2005).
[12] L. Shan, Y. Huang, H. Gao, Y. Wang, S. L. Li, P. C. Dai, F. Zhou, J. W. Xiong, W. X. Ti, and H. H. Wen, Phys. Rev. B **72**, 144506 (2005).
[13] I. Eremin, E. Tsoncheva, and A. V. Chubukov, Phys. Rev. B **77**, 024508 (2008).
[14] B. S. Chandrasekhar and D. Einzel, Annalen der Physik **505**, 535 (1993).
[15] W. S. Lee, I. M. Vishik, K. Tanaka, D. H. Lu, T. Sasagawa, N. Nagaosa, T. P. Devereaux, Z. Hussain, and Z.-X. Shen, Nature **450**, 81 (2007).
[16] T. Kondo, A. D. Hamaya, Yoichiro Palczewski, T. Takeuchi, J. S. Wen, G. Xu, Z. J. Gu, J. Schmalian, and A. Kaminski, Nat. Phys. **7**, 21 (2011).
[17] I. M. Vishik, M. Hashimoto, R.-H. He, W.-S. Lee, F. Schmitt, D. Lu, R. G. Moore, C. Zhang, W. Meevasana, T. Sasagawa, S. Uchida, K. Fujita, S. Ishida, M. Ishikado, Y. Yoshida, H. Eisaki, Z. Hussain, T. P. Devereaux, and Z.-X. Shen, PNAS **109**, 18332 (2012).
[18] I. M. Vishik, Rep. Prog. Phys. **81**, 062501 (2018).
[19] D. M. Broun, D. C. Morgan, R. J. Ormeno, S. F. Lee, A. W. Tyler, A. P. Mackenzie, and J. R. Waldram, Phys. Rev. B **56**, R11443 (1997).
[20] W. Anukool, S. Barakat, C. Panagopoulos, and J. R. Cooper, Phys. Rev. B **80**, 024516 (2009).
[21] S.-F. Lee, D. C. Morgan, R. J. Ormeno, D. M. Broun, R. A. Doyle, J. R. Waldram, and K. Kadowaki, Phys. Rev. Lett. **77**, 735 (1996).

Copyright © 2024